Exploiting natural polysaccharides to enhance in vitro bio-constructs of primary neurons and progenitor cells

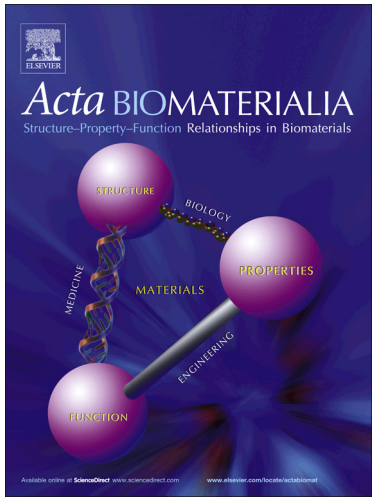


Full length article

# Exploiting natural polysaccharides to enhance *in vitro* bio-constructs of primary neurons and progenitor cells

Manuela Medelin, Davide Porrelli, Emily Rose Aurand, Denis Scaini, Andrea Travan, Massimiliano Antonio Borgogna, Michela Cok, Ivan Donati, Eleonora Marsich, Chiara Scopa, Raffaella Scardigli, Sergio Paoletti, Laura Ballerini

PII: S1742-7061(18)30172-7
DOI: https://doi.org/10.1016/j.actbio.2018.03.041
Reference: ACTBIO 5383

To appear in: *Acta Biomaterialia*

Received Date: 8 December 2017
Revised Date: 23 February 2018
Accepted Date: 26 March 2018

Please cite this article as: Medelin, M., Porrelli, D., Aurand, E.R., Scaini, D., Travan, A., Borgogna, M.A., Cok, M., Donati, I., Marsich, E., Scopa, C., Scardigli, R., Paoletti, S., Ballerini, L., Exploiting natural polysaccharides to enhance *in vitro* bio-constructs of primary neurons and progenitor cells, *Acta Biomaterialia* (2018), doi: https://doi.org/10.1016/j.actbio.2018.03.041

# Exploiting natural polysaccharides to enhance *in vitro* bio-constructs of primary neurons and progenitor cells

**Authors**

Manuela Medelin[a,b], Davide Porrelli[a†], Emily Rose Aurand[a], Denis Scaini[a,c], Andrea Travan[a], Massimiliano Antonio Borgogna[a], Michela Cok[a], Ivan Donati[a], Eleonora Marsich[d], Chiara Scopa[e], Raffaella Scardigli[f,g*], Sergio Paoletti[a*] & Laura Ballerini[b*]

**Affiliations**

[a] Department of Life Sciences, University of Trieste, 34127 Trieste, Italy.

[b] International School for Advanced Studies (SISSA/ISAS), 34136 Trieste, Italy.

[c] ELETTRA Sincrotrone Trieste S.c.p.A., 34149 Trieste, Italy.

[d] Department of Medical, Surgical and Health Sciences, University of Trieste, 34125 Trieste, Italy.

[e] University of Rome "Roma Tre", 00154 Rome, Italy.

[f] Institute of Translational Pharmacology, National Research Council (IFT-CNR), 00133 Rome, Italy.

[g] European Brain Research Institute (EBRI), 00143 Roma, Italy.

*Corresponding authors:

Laura Ballerini: laura.ballerini@sissa.it; Sergio Paoletti paolese1@gmail.com; Raffaella Scardigli r.scardigli@ebri.it

[†] Present address: Department of Medical, Surgical and Health Sciences, University of Trieste, 34125 Trieste, Italy.

**Abstract**

Current strategies in Central Nervous System (CNS) repair focus on the engineering of artificial scaffolds for guiding and promoting neuronal tissue regrowth. Ideally, one should combine such synthetic structures with stem cell therapies, encapsulating progenitor cells and instructing their differentiation and growth. We used developments in the design, synthesis, and characterization of polysaccharide-based bioactive polymeric materials for testing the ideal composite supporting neuronal network growth, synapse formation and stem cell differentiation into neurons and motor neurons. Moreover, we investigated the feasibility of combining these approaches with engineered mesenchymal stem cells able to release neurotrophic factors. We show here that composite bio-constructs made of Chitlac, a Chitosan derivative, favor hippocampal neuronal growth, synapse formation and the differentiation of progenitors into the proper neuronal lineage, that can be improved by local and continuous delivery of neurotrophins.

Statement of Significance

In our work, we characterized polysaccharide-based bioactive platforms as biocompatible materials for nerve tissue engineering. We show that Chitlac-thick substrates are able to promote neuronal growth, differentiation, maturation and formation of active synapses. These observations support this new material as a promising candidate for the development of complex bio-constructs promoting central nervous system regeneration. Our novel findings sustain the exploitation of polysaccharide-based scaffolds able to favour neuronal network reconstruction. Our study shows that Chitlac-thick may be an ideal candidate for the design of biomaterial scaffolds enriched with stem cell therapies as an innovative approach for central nervous system repair.

**Keywords**

Chitosan, Chitlac, CTL, polysaccharide, coatings, functional synaptic networks, hippocampal neurons, neuronal progenitors, mesoangioblasts, neurotrophins, patch-clamp, immunofluorescence, layer-by-layer deposition, contact angle.

## 1. Introduction

In the adult, CNS lesions usually result in permanent functional deficits due to the limited self-repair capacity of the brain and the spinal cord. Innovative approaches are continuously explored to improve regeneration of the damaged CNS and the combination of biomaterial scaffolds with stem cell therapies emerges as one of the more promising. Stem cells of different origins, such as embryonic (ESCs), neural (NSCs), mesenchymal (MSCs) and, more recently, induced pluripotent stem cells (iPSCs), are engineered in cell-based therapies, also to provide sources of signaling molecules, including anti-inflammatory cytokines and growth factors [1]. Further combined research in biomaterial science and neurobiology is needed to tailor bioactive composites with properties that, once engineered into scaffolds, can guide or favor the growth of encapsulated progenitor cells or interfaced neurons. The properties of biomaterials can influence cell functions; in particular, wettability and hydrophilicity of surfaces are important parameters promoting cell adhesion and growth [2]. In fact, in addition to chemical and spatial cues, physical features of the substrate, such as gradients in surface energy, may impact on cell biology (*e.g.* neuronal differentiation of PC12 cells) and should be considered when designing novel biomaterials [3].

In this arena, the use of polysaccharides represents a novel and promising strategy. These macromolecules are structural components of, among others, the hydrated extracellular matrix (ECM), crucial to ECM biomechanical performances and responses to stressors [4]. Charged polysaccharides are also used to functionalize surfaces *via* layer-by-layer deposition approach [4-6]. Among charged polysaccharides, Chitosan and its derivatives have received particular attention.

Chitosan is a biocompatible polycation derived from the deacetylation of chitin and it has been studied for several biomedical applications, including tissue engineering, wound dressing and drug delivery [7]. In particular, for neural tissue engineering, Chitosan has been used for the preparation of hydrogels, nanofibers and oriented porous scaffolds, as neuron and growth factor carriers, or as substrates for neurons proliferation and differentiation [8-12]. The use of Chitosan is usually combined to growth factors or polymers to enhance its biological performance [13-15]. The derivation of Chitosan with lactose moieties enables for the preparation of an engineered polysaccharide (Chitlac) with improved solubility, able to trigger biological events in chondrocytes and osteoblasts [4,16-17]. Due to its peculiar chemical features, Chitlac can interact with polyanions, such as alginate or hyaluronic acid [18]. To note, the possibility to combine Chitlac with alginate allows preparing biomaterials in the form of hydrogels [19] or porous scaffolds [17], in which alginate plays the structural role and Chitlac the bioactive one. In this framework, alginate can be exploited to manufacture porous scaffolds with aligned channels [20], potentially useful to guide the growth of axons and their orientation within the scaffold.

In this work, we present results on the characterization of the morphology, hydrophilicity and surface energy of different bio-platforms based on Chitosan and Chitlac, respectively, to favor neuronal differentiation and growth. We developed four

substrates for cell growth characterized by Chitosan or Chitlac in thin or enriched layers. The ability of these different substrates to promote the reconstruction of synaptic active networks when interfacing with cultured postnatal brain neurons was tested by immunofluorescence, microscopy and electrophysiology. We further challenged the most promising substrates with cortical and spinal cord progenitor cells, to measure the ability of these biomaterials to promote stem cell differentiation into cortical neurons and motor neurons. Finally, we increased the level of complexity of the bio-construct by implementing the system with mesenchymal stem cells, *i.e.* mesoangioblasts (MABs), engineered to release neurotrophic factors and combined with the different substrates.

## 2. Materials and Methods

### 2.1. Materials

Chitosan was purchased from Sigma-Aldrich and purified as reported [18]. Chitlac (lactose-modified chitosan, or CTL, CAS registry number 2173421-37-7) was prepared according to the procedure reported elsewhere [21], starting from a highly deacetylated Chitosan (residual acetylation degree approximately 11%). The (viscosity average) relative molar mass of Chitosan was estimated to be approximately $7\times10^5$. The monomer composition of Chitlac was determined by means of $^1$H NMR and resulted to be: glucosamine = 24%; N-acetylglucosamine = 11%; and 2-(lactit-1-yl)-glucosamine = 65%. The relative molecular mass, MW, of Chitlac was estimated to be approximately $1.5\times10^6$. Alginate was provided by FMC (LVG type, MW = 120 000; $F_G = 0.69$; $F_{GG} = 0.59$; $N_{G>1} = 16.3$. $F_G$, $F_{GG}$, and $N_{G>1}$ are the fraction of guluronic acid (G) co-monomer, the fraction of G dyads and the average length of homopolymeric sequences of - at least two - G co-monomers, respectively).

**2.2. Preparation of fluorescein-labeled polymers**

200 mg of Alginate were dissolved in 70 mL of MES buffer (Sigma-Aldrich, 50 mM; pH 5.5). Fluoresceinamine (Sigma-Aldrich, 1 mg/mL in methanol) was added to the Alginate solution to label one over 500 of available carboxylic groups. Next, an amount of EDC (1.5 times the monomeric units of alginate) and of NHS (1:1 with EDC) were added to the solution. The reaction mixture was stirred 2 hours at room temperature (RT). Next, the mixture was dialyzed (dialysis membrane Spectrapore, MWCO 12 000) three times against $NaHCO_3$ 0.05 M, two times against NaCl 0.1 M and against deionized water until the conductivity of the external solution was below 2 µS at 4 °C. All procedures were carried out under dark conditions. The pH was adjusted to a value between 6.8 and 7.2 and then the solution was filtered through 0.45 µm filters and freeze-dried.

90 mg of Chitosan in 30 mL of deionized water (pH was adjusted to 5.5 with HCl). Then 200 µL of a Fluorescein-isothiocyanate (FITC, Sigma-Aldrich) solution (0.5 mg/mL in sodium carbonate buffer, 0.5 M) were added to the solution. The reaction mixture was stirred 24 hours at room temperature. Next, the mixture was dialyzed (dialysis membrane Spectrapore, MWCO 12 000) three times against $NaHCO_3$ 0.05 M, two times against NaCl 0.1 M and against deionized water until the conductivity of the external solution was below 2 µS at 4 °C. All procedures were carried out under dark conditions, the pH was adjusted to 4.5 and then the solution was filtered through 0.45 µm filters and freeze-dried.

200 mg of Chitlac were dissolved in 70 mL sodium carbonate buffer (0.5 M). 20 µL of a FITC solution in the same buffer (5 mg/mL) were added drop wise to the Chitlac solution to label one over 2 000 available amino groups. Next, the mixture was dialyzed (dialysis membrane Spectrapore, MWCO 12 000) three times against

$NaHCO_3$ 0.05 M, two times against NaCl 0.1 M and against deionized water until the conductivity of the external solution was below 2 μS at 4 °C. All procedures were carried out under dark conditions. The solution was filtered through 0.45 μm filters and freeze-dried.

**2.3. Activation and coating of glass coverslips**

Glass coverslips (O. Kindler GmbH) were treated with piranha solution ($H_2SO_4$:$H_2O_2$ 30% = 3:1) at 80 °C for 1 hour, thoroughly washed with deionized water and methanol and finally air-dried. In order to prepare the thin layer coated coverslips, after the activation with the piranha solution, Chitlac or Chitosan were placed onto the coverslips. Chitlac was solubilized in HCl (at pH = 4.5), Chitosan was solubilized in acetic acid 0.02 M and Alginate was solubilized in deionized water. All polysaccharide solutions have been used at the concentration of 5 mg/mL. For each coating step, 200 μL of polymer solution were poured onto the activated glass coverslip. After 1 hour of incubation at RT, the excess of the solution was removed and the coverslips were washed twice for 1 hour with HEPES (10 mM, pH = 7.4). The coverslips were washed with deionized water and air-dried. The two samples have been called Chitosan-THIN and Chitlac-THIN, respectively.

In order to prepare the enriched coated coverslips, after the activation with the piranha solution, Chitlac or Chitosan were placed on the coverslips. After 1 hour of incubation at RT, the excess of the solution was removed and the coverslips were washed with deionized water (pH 4.5) or acetic acid 0.02 M (pH 3.2), respectively, and dried in air. Polycation/polyanion electrostatic interactions were exploited to improve the substrate thickness. To this end, a layer of Alginate (polyanion) was placed onto the coverslips coated with Chitlac or Chitosan (polycations) and incubated (RT, 1 hour). The excess of Alginate solution was removed; then the coverslips were washed with deionized

water and finally air-dried. Finally, additional Chitlac or Chitosan solution was placed to top up the coverslips. After 1 hour of incubation at RT, the excess of the solution was removed and the coverslips were washed twice for 1 hour with HEPES (10 mM, pH = 7.4). The coverslips were washed with deionized water and air-dried. These surfaces have been indicated as Chitosan-THICK and Chitlac-THICK, respectively.

**2.4. Confocal microscopy and Atomic Force Microscopy (AFM)**

Coated glass coverslips were prepared labeling only one of the polymers composing the coating. The coverslips were prepared in dark conditions and mounted on microscope slides with Mowiol 4-88 (poly(vinyl alcohol)). Images were taken with a Nikon Eclipse C1 microscope, with an objective Nikon Plan Fluor 20× (0.5 NA, dry) using argon laser (488 nm) and acquisition channel of 515/30 nm. Images were analyzed with ImageJ software. For the confocal microscopy analysis, the glass substrates have been coated with fluorescein-labeled Chitosan, Chitlac and/or Alginate, according to the procedure reported above; in the case of enriched layers (Chitosan-THICK or Chitlac-THICK), only one labeled polymer per sample was used. Figure S1 of the Supplementary Material collects the confocal images of the four different surfaces.

Polysaccharide-coated glass surfaces were measured using atomic force microscopy (AFM) in order to determine dry film thickness. Pristine samples were mounted on magnetic plates using double-side adhesive tape. AFM was used in dynamic mode at RT in air using a commercial instrument (Solver Pro, NT-MDT, RUS). Silicon tips (NSC16/NoAl series probes from MikroMasch, USA) with a typical force constant of 45 nN/nm and a typical resonance frequency of about 190 kHz were employed. The thicknesses of the polysaccharide films were determined measuring the height between the top of the film and the underneath glass in correspondence with scalpel-

made scratches where the film was removed. Glass surface was used as height reference. Topographic height images were recorded at 512 × 512 pixels at a scan rate of 1 Hz. All image processing was performed using Gwyddion freeware AFM analysis software [22].

**2.5. Contact angle studies**

Contact angles of the surfaces were measured using a Microscope Leica MZ16 equipped with a camera Leica DFC320 using the sessile drop method [23]. Both polar (ultrapure water and ethylene glycol) and non-polar (ultrapure diiodomethane) liquids were used in order to allow surface energy calculations. A droplet of liquid (4 μL) was placed on the surface. The profile of the water drop on the surface was recorded after 10 seconds to avoid time-dependent angle variations among samples. Contact angles were measured by image analysis software (Image Pro Plus 6.2). For statistical analysis, 10 measurements for each surface type were averaged. The surface energy parameters were calculated from the contact angle values of the probe liquids according to the acid−base method proposed by Van Oss [24]. Briefly, the values of the contact angles of the three liquids were used in the Young−Duprè equation ($(1 + \cos\theta) \cdot \gamma_l = 2[(\gamma_s^{LW} \cdot \gamma_l^{LW})^{1/2} + (\gamma_s^{+} \cdot \gamma_l^{-})^{1/2} + (\gamma_s^{-} \cdot \gamma_l^{+})^{1/2}]$), where $\gamma_l$ and $\gamma_s$ are the free energies of the liquid and the solid, respectively. This equation enables one to calculate the values of the Lifshitz-van der Waals contribution of surface tension, $\gamma^{LW}$, and the acid−base (AB) components $\gamma^{+}$ and $\gamma^{-}$ of the material. The surface polarity was calculated as the ratio between the AB contribution and the total surface tension $\gamma^{tot}$ ($\gamma^{tot} = \gamma^{LW} + \gamma^{AB}$, where $\gamma^{AB} = (\gamma_s^{+} \cdot \gamma_l^{-})^{1/2}$). Considering the thermodynamic work of adhesion between surface and liquids, the total work is given by $W^T = W^{AB} + W^{LW}$ where $W^{AB} = (1 + \cos\theta) \cdot \gamma_l - 2 \cdot [(\gamma_s^{LW} \cdot \gamma_l^{LW})^{1/2}]$ and $W^{LW} = 2 \cdot [(\gamma_s^{LW} \cdot \gamma_l^{LW})^{1/2}]$,

while the $W^{AB}$ (%)is obtained by dividing $W^{AB}$ by $W^{T}$ ( × 100). More details on the calculations can be found in Travan *et al.* [25].

**2.6. Cell culture**

Primary cultures of hippocampal neurons were obtained from 2 or 3 days postnatal (P2-P3) rat pups as previously reported [26-29]. Briefly, hippocampi were isolated and cells were dissociated enzymatically and mechanically. Cells were plated (150 µL of cell suspension) on four different substrates: Chitosan-THIN, Chitlac-THIN, Chitlac-THICK and Chitosan-THICK, respectively. 30 000 cells were plated on each coverslip (12 × 24 $mm^2$, between 0.13 and 0.16 mm thick, Kindler, EU). Chitosan-THIN was selected as the control condition. In fact, Chitosan biocompatibility has been reported in previous works *in vitro* [12,30] and *in vivo* [13-15,31]. In our experiments, neurons grown on Chitosan-THIN displayed core functional properties (such as the frequency and amplitudes of post synaptic currents, PSCs, and those of miniature PSCs, Figure 2 C, D and F) within the range of values usually measured in hippocampal cultures grown on poly-L-ornithine [32-33]. Cultures were incubated at 37 ºC, in a humidified atmosphere with 5% $CO_2$ in culture medium. It was a minimum essential medium (MEM; from Gibco® - ThermoFisher Scientific) containing also: 35 mM glucose (Carlo Erba Reagents), 15 mM HEPES, 1 mM Apo-Transferrin, 48 µM Insulin, 3 µM Biotin, 1 mM Vitamin B12 (all from Sigma-Aldrich) and 500 nM Gentamicin (Gibco® - ThermoFisher Scientific) in the presence of 10% dialyzed fetal bovine serum (FBS, Invitrogen). Culture medium (supplemented with cytosine-arabinoside Ara C, a proliferation inhibitor, and with a lower concentration of serum, 5%) was renewed (60% medium replacement) after two days from seeding and changed every two days. Cultures were then used for experiments after 8 to 10 days *in vitro* (DIV).

Fetal neural progenitor cells (fNPCs) were derived from embryonic day 15 (E15) rats as reported [34]. Briefly, embryos from timed pregnant females were excised into cold Gey's Balanced Salt Solution (GBSS) and decapitated. Whole brains, minus the olfactory bulbs and cerebella, were washed three times in ice cold GBSS. Tissues were mechanically dissociated to single cell suspension by using first a 10 mL pipette tip, followed by a 1 mL pipette tip. The cell solution was divided into uncoated Petri dishes with cells from approximately three brains per dish. Cells were cultured as neurospheres at 37 °C and 5% $CO_2$, in a humidified chamber, in standard serum-free medium 3:1 DMEM/F12 (Sigma-Aldrich). It also contained 1 × B27 supplement (Life Technologies), 100 U/mL penicillin (Fisher Scientific), 1 µg/mL streptomycin (Fisher Scientific), 2 mM L-Glutamine (Fisher Scientific), and 20 ng/mL each basic fibroblast growth factor (bFGF, Invitrogen) and epidermal growth factor (EGF, Invitrogen). One-half of the culture medium was replaced every other day. Five days after isolation (DIV5), neurospheres were dissociated and the cell suspension was plated on the different substrates. Approximately 30000 cells were plated on each coverslip consisting of Chitosan-THIN, Chitlac-THIN and Chitlac-THICK. Cultures were incubated at 37 °C, in a humidified atmosphere with 5% $CO_2$ in differentiation medium, consisting of 1:1 DMEM/F12, 100 U/mL penicillin, 1 µg/mL streptomycin, 2 mM L-glutamine, and 10% FBS. Plates were incubated at 37 °C and 5% $CO_2$. No additional growth factors were added to direct NPC differentiation towards a specific cell fate. Half of the differentiation medium was replaced every other day. Cultures were then used for immunocytochemistry experiments after two weeks *in vitro* (WIV).

D7 motor neuron (MN) progenitors were derived from embryonic spinal cord as previously described [35]. Cells were cultured as neurospheres in DMEM/F12

medium supplemented with B27 (Invitrogen), EGF and bFGF (20 and 10 ng/mL, respectively; Peprotech) (growing medium) in a humidified incubator at 37°C in 5% $CO_2$. To assess differentiation, neurospheres were dissociated into single cells and then transferred onto Chitosan-THIN, Chitlac-THIN and Chitlac-THICK layers, respectively. It was done in differentiating medium (growth medium without EGF and FGF) at $5 \times 10^4$ cells density, in co-culture with control or neurotrophins producing mesoangioblasts (MABs) at the same cell density. Seven days after plating, cultures were fixed in 4% formaldehyde (prepared from fresh paraformaldehyde) in PBS and processed for immunocytochemistry.

GFP-expressing MABs D16, "clone D16", were grown in DMEM plus 10% FBS as described [36]. NGF-expressing MABs (D16-NGF, "clone F10") and BDNF-expressing MABs (D16-BDNF, "clone A9") have been obtained upon stable transfection of D16 cells and single clone selection, as described in Su *et al.* (2012). F10 and A9 MABs produce 36 ng/mL/day/$10^6$ cells of NGF and 30 ng/mL/day/$10^6$ cells of BDNF, respectively [37].

In the co-cultures (primary neurons and control or neurotrophins producing MABs), hippocampal neurons were cultured as previously described. A 1:1 ratio between the two cell populations was maintained. Thereafter, 30 000 cells for each type of MABs were dissolved into the dissociated hippocampal neuron medium. These co-cultures were tested on the Chitlac-THICK substrate. In this set of experiments "control", "D16-MABs", "A9-MABs BDNF" and "F10-MABs NGF" refer to dissociated hippocampal cultures alone, co-culture with control MABs, co-culture with BDNF-producing MABs and co-culture with NGF-producing MABs, respectively.

**2.7. Electrophysiological recordings**

For patch clamp recordings (whole-cell, voltage clamp mode performed at RT), the

samples were positioned in a recording chamber, mounted on an inverted microscope and continuously superfused with control physiological saline solution containing (mM): 150 NaCl, 4 KCl, 2 $CaCl_2$, 1 $MgCl_2$, 10 HEPES and 10 glucose. The pH was adjusted to 7.4 with NaOH (osmolarity: 300 mOsm). Cells were patched with pipettes (4 to 7 MΩ) filled with a solution of the following composition (mM): 120 potassium gluconate, 20 KCl, 2 $MgCl_2$, 2 $Na_2ATP$, 10 HEPES and 10 EGTA. pH was adjusted to 7.3 with KOH (osmolarity: 295 mOsm). Voltage values indicated in the text and in the figures have not been corrected for the liquid junction potential, estimated to be ~ 14 mV [38]. Electrophysiological responses were amplified (EPC-7, HEKA; Multiclamp 700B, Axon Instruments), sampled and digitized at 10 kHz with the pClamp software (Axon Instruments) for offline analysis. Single spontaneous synaptic events were detected by the use of the AxoGraph X (Axograph Scientific) event detection program [39]. On average, ≥ 400 events were analyzed for each cell in order to obtain mean parameters. Neuronal passive properties were measured by repeated (80 times) stimulation of cells with a 100 ms lasting hyperpolarizing stimulus (5 mV). The area below capacitive transients was computed and normalized for voltage transient amplitude to calculate cell capacitance ($C_m$). Input resistance ($R_{in}$) was obtained through Ohm's law, by measuring the amplitude of steady state current generated by the voltage transient. In order to remove action potential-dependent currents, tetrodotoxin (TTX; Latoxan) was bath-applied at the concentration of 1 μM, thus allowing recording miniature PSCs (mPSCs).

**2.8. Immunocytochemistry, image acquisition and analysis**

Immuno-labeling on dissociated hippocampal neurons was performed after fixation with 4% formaldehyde (prepared from fresh paraformaldehyde) in PBS for 20 min at room temperature. Cells were permeabilized and blocked in 5% FBS and 0.3% Triton

X-100 for at least 30 min at RT and incubated with the following primary antibodies for 30 min: rabbit polyclonal anti- β-Tubulin III (Sigma-Aldrich, T2200, 1:500) and mouse monoclonal anti-glial fibrillary acid protein (GFAP; Sigma-Aldrich, G3893, 1:250). Upon washing, cells were then incubated for 30 min with the following secondary antibodies: goat anti-rabbit Alexafluor 594 (Invitrogen, A-11012, 1:500), goat anti-mouse Alexafluor 488 (Invitrogen, A-11001, 1 : 500) and 4, 6-diamidine-2-phenylindole dihydrochloride (DAPI, Invitrogen, D1306, 1 : 200) to label the nuclei. Finally, samples were washed in PBS and quickly rinsed with MilliQ water to remove the PBS salt residual and mounted on glass microscope slides using Vectashield® hard set mounting medium (Vector Laboratories). Fluorescence images were acquired using a Leica DM6000 upright microscope with a 20 × dry objective (field size 713 x 533 $\mu m^2$). Identical binning, gains and exposure times were used for all images of the same marker. Image analysis was performed using the professional image analysis software Volocity (PerkinElmer). For the quantification of the β-Tubulin III positive area, a threshold was set for both intensity and object size, thus ensuring that the observed signal indicates the presence of genuine β-Tubulin III positive labeling [40]. Fluorescence intensity was quantified using Fiji [41]. Cell density counting analysis (number of cells/$mm^2$) was performed by merging the DAPI with the β-Tubulin III signal (for neuronal density) or with the GFAP signal (for glial density). This allowed visualizing double positive cells for nuclei and β-Tubulin III or GFAP, respectively. We measured at least three fields randomly selected from each sample per condition.

To identify fNPCs that differentiated into either astrocytes or neurons, all coverslips were processed for immunocytochemistry. The procedure was similar to that described for dissociated hippocampal neurons. To label astrocytes and neurons, mouse monoclonal anti-GFAP and rabbit polyclonal anti-β-Tubulin III were used,

respectively. To identify more mature neurons, mouse monoclonal anti-MAP2 (Sigma-Aldrich, M9942, 1:250) was used. Goat anti-rabbit Alexafluor 594 and goat anti-mouse Alexafluor 488 were used as secondary antibodies. All cell nuclei were labeled with DAPI.

To assess the number of cells present on each substrate after 2WIV, the total number of DAPI-positive cells was counted per image and used to determine the average density of cells per $mm^2$. To assess differentiation, the following marker-positive area values were assessed: β-Tubulin III for neurons, GFAP for glia/astrocytes and MAP2 for mature neurons. Differentiation data have then been reported as β-Tubulin III and GFAP area as a percentage of the total area and, for mature neurons, as a ratio of MAP2/ β-Tubulin III positive area.

Immuno-labeling on D7 MN progenitors was performed after fixation in 4% formaldehyde (prepared from fresh paraformaldehyde) in PBS for 10 min at RT. Upon fixation, cells were permeabilized in 0.1% Triton X-100 in PBS and then incubated with the following primary antibodies: rabbit polyclonal anti-GFAP (DakoCytomation, Z0334, 1:250), mouse monoclonal anti-Neuronal class III β-Tubulin (Covance; MMS-435P, 1:250), goat polyclonal anti-choline acetyltransferase (ChAT) (Merck Millipore, AB144P, 1:200). Incubation then followed with secondary antibodies: goat-anti rabbit antiserum conjugated to Alexafluor 488 (Invitrogen), goat-anti mouse antiserum conjugated to Alexafluor 594 (Invitrogen), donkey anti-goat conjugated to Alexa 647 (Invitrogen). Immuno-labeled cells were mounted in Aqua-Poly/Mount (Polysciences, Inc.) and analyzed at confocal microscopy, using a TCS SP5 microscope (Leica Microsystem). Z-stacks images were captured at 1-µm intervals with a 40× or 63× objectives (N.A. 1.25 or 1.40) and a pinhole of 1.0 Airy unit. Analyses were performed in sequential scanning mode to rule out cross bleeding

between channels. Fluorescence intensity quantification of β-Tubulin III was performed with ImageJ software. To quantify the percentage of differentiation, the number of β-Tubulin III and GFAP immunoreactive cells was counted in at least ten non-overlapping fields in each sample, for a total of > 1000 cells per sample. The total number of cells in each field was determined by counterstaining cell nuclei with DAPI (Sigma-Aldrich, 50 mg/mL in PBS for 15 min at RT). The average percentage of differentiated cells for each sample was then calculated by dividing the number of Tuj1 and GFAP positive cells by the total number of cells for each field. For motor neuron differentiation, the number of β-Tubulin III and ChAT immunoreactive cells was counted in at least ten non-overlapping fields (40× magnification, each field measuring 0.15 $mm^2$, corresponding to 7.5% of the whole coverslip area), counting 5 to 30 ChAT positive cells, depending on the sample. Then the average percentage of ChAT positive cells was calculated by dividing the number of ChAT immunoreactive cells a by the total number of β-Tubulin III positive cells for each field. Data are the mean ± SD of three independent cultures, three independent experiments for each culture.

**2.9. Statistical analysis**

Results are presented as mean ± standard deviation (SD) or through box-plot representations. In box-plots, the thick horizontal bar indicates the median value, the boxed area extends from the $25^{th}$ to $75^{th}$ percentiles while whiskers from the $5^{th}$ to the $95^{th}$ percentiles. The homogeneity of variances was assessed through the Levene's test; n is the number of neurons, if not otherwise indicated. One-way analysis of variance (one-way ANOVA) was used to determine significance when multiple groups were compared and Fisher's least significant difference was used to determine

significance post hoc. $P < 0.05$ was accepted as indicative of a statistically significant difference.

### 2.10. Ethical Statement

All animal procedures were conducted in accordance with the National Institutes of Health, international and institutional standards for the care and use of animals in research, and after consulting with a veterinarian. All experiments were performed in accordance with the EU guidelines (2010/63/UE) and Italian law (decree 26/14) and were approved by the local authority veterinary service. All efforts were made to minimize animal suffering and to reduce the number of animal used. The Italian Ministry of Health, in agreement with the EU Recommendation 2007/526 /CE, approved animal use.

## 3. Results

The aim of this work is to compare the suitability of the Chitosan derivative named Chitlac - as compared with that of its parent polymer - to favor neuronal differentiation and growth. Among the techniques used for the critical assessment of the ability of these substrates to promote the reconstruction of synaptic active networks, electrophysiology presents some stringent technical requirements. In particular, it makes it necessary to use suitable glass coverslips to firmly supporting the biomaterial (that in turn nests the observed neurons). For this reason, the first set of experiments aimed at producing the best conditions allowing for the deposition of the polysaccharides, the growth of neurons and the carrying on of the electrophysiological experiments.

### 3.1. Functionalization of substrates with Chitosan and Chitlac

In order to evaluate the effect of Chitlac and of its parent compound Chitosan, the glass coverslips were coated by deposition of the cationic polysaccharides, upon pre-treatment (anionization) of the surfaces with piranha solution (see Materials and Methods). The deposition was driven by electrostatic interactions between the positive charges on the polysaccharides and the negative charges introduced on the glass coverslips. The thickness of the dry layers of the two polysaccharides was determined by means of Atomic Force Microscopy (AFM). The measured values were 5 ± 2 nm for Chitlac and 104 ± 24 nm for Chitosan.

The layers, albeit dehydrated, obtained through the sole activation of the glass surface were very thin, especially in the case of Chitlac. In order to increase the thickness of the layers, we resorted to use Alginate. This negatively charged polysaccharide is known to be biologically inert and it has been shown to favor the adsorption of positively charged polysaccharides over surfaces and within bulk structures, both in solution [42] and in the gel state [17]. Alginate adsorbed onto the first, thin layer of polysaccharide by means of electrostatic interactions. Due to the high density of negative charges contributed by the polyanion, the additional deposition of Chitlac or Chitosan led to an increase of the amount of the cationic polysaccharide composing the modified surface of the glass coverslips. The result is a highly interpenetrated layer enriched in the polycation (see Scheme 1).

The increase of the dehydrated layer of polycations was again measured by means of AFM, which showed a thickness of 24 ± 18 nm and 213 ± 32 nm for Chitlac-THICK and Chitosan-THICK surfaces, respectively. The efficacy of the approach was then clearly demonstrated, in particularly so for the relative increase of adsorbed Chitlac.

Polysaccharides, and particularly so Chitlac [43], are able to absorb a large amount of water, which is the operational condition of application of the biomaterials and of all

the following biological experiments. To this end, we decided to quantify such tendency and, more generally, the polymer/water interactions. Contact angle studies were performed to evaluate the wettability of the coated surfaces. The values obtained are reported in the Table S1 (Supporting Information) and show that the contact angles of water on the modified surfaces enriched in polycation thin layers significantly (** $P < 0.01$) decreased when Chitlac replaced Chitosan: from $68 \pm 6$ to $45 \pm 5$, respectively (plotted in Figure 1A), pointing at the higher wettability of Chitlac-based coatings.

The surface energies of the polysaccharide-coated surfaces were calculated from contact angle measurements according to the Van Oss theory, by means of the Young-Duprè equation [24]. The surface energy parameters and work of adhesion are reported in the Table S2 (Supporting Information). The total surface energy $\gamma^{TOT}$ of the four different surfaces ranges from 43.0 to 50.2 $mJ/m^2$, in line with previous investigations on polysaccharide-coated methacrylate-based surfaces [25]. In the case of the Chitlac-THICK coating, the higher value of the acid-base interactions ($\gamma^{AB}$) causes a considerable increase in the surface polarity with respect to the Chitosan-THICK coating (Chitlac-THICK: 16.7%, Chitosan-THICK: 11.5%; ** $P < 0.01$). Table S2 shows also that the presence of Chitlac is associated with a significant (** $P < 0.01$) increase of acid−base interactions with water: from 40 $mJ/m^2$ to 64 $mJ/m^2$ for polycation-enriched layers with Chitlac and Chitosan, respectively (plotted in Figure 1B); at variance, the dispersive contribution ($\gamma^{LW}$) is almost constant among all the surfaces.

**3.2. Effect of polysaccharide-coated surfaces on neuronal growth and synapse formation**

We tested the newly engineered substrates ability to sustain neuronal growth *in vitro* [44]. To evaluate how brain cells reacted to the polymeric matrices, we grew dissociated hippocampal cells where neurons and glial cells were directly put in contact with the different polymers. After 8 to 10 days of *in vitro* growth, we performed immunofluorescence labeling and electrophysiological recordings to estimate cell viability, morphology and activity. The tests were performed both on polycation-coated substrates and on polycation-enriched substrates.

As a premise, it should be underlined that cells barely grew or did not grow at all on the Chitosan-THICK substrates (not shown; n = 4 culture series). The most likely explanation is because Chitosan and Alginate are incompatible polymers: these unbranched, oppositely charged polyelectrolytes normally give rise to coalescence, phase separation and precipitation, thus making a very unfriendly environment for cells.

This consideration marks immediately the difference between the two polycations: Chitlac, albeit bearing positive charges like Chitosan, is surprisingly able to be miscible ("compatible") with polyanions [42], like Alginate or Hyaluronan. This is due to the lactitol side-chain branching which forbids close contact of its positive charges with the negative ones of the opposite polyanion, thus stressing its positive role as a versatile modified version of Chitosan.

Three polymer combinations, Chitosan-THIN, Chitlac-THIN and Chitlac-THICK, allowed cell attachment and growth (Figure 2A; n = 25 culture series) and were further investigated.

The patterns of hippocampal cell distribution (GFAP-positive glial cells and β-Tubulin III-positive neurons, Figure 2A) varied when comparing the three different substrates. When Chitosan-THIN was used as a coating, cells usually appeared as

aggregated in clusters (Figure 2A left panel), at variance with the evenly distributed morphology observed in Chitlac-THIN and Chitlac-THICK cultures (Figure 2A middle and right panels, respectively). We did not quantify these different patterns, but we quantified the total number of neurons or glial cells (by DAPI co-labeling with β-Tubulin III or with GFAP, respectively, expressed as cells/mm$^2$) measuring ≥ 3 visual fields (713 × 533 μm$^2$) randomly selected from each slide. Regardless of their being in clusters or more distributed within each field, hippocampal neurons showed a comparable survival rate when investigated after 10 days of *in vitro* growth. In fact, they showed similar values of density (neurons/mm$^2$) (see Table 1A).

**Table 1.** - Neuronal growth on polysaccharide-coated surfaces

| | **A** | | **B** | **C** | **D** |
|---|---|---|---|---|---|
| **SUBSTRATES** | number of neurons | | total β-Tubulin III-positive area | number of GFAP positive glial cells | GFAP positive areas |
| | *neurons/mm$^2$* | | *μm$^2$* | *astrocytes/mm$^2$* | *μm$^2$* |
| Chitosan-THIN | 223 ± 110 | n = 11 | (56 ± 20) ×10$^3$ | 91 ± 23 | (51 ± 17) ×10$^3$ |
| Chitlac-THIN | 241 ± 87 | n = 19 | (99 ± 34) ×10$^3$ | 117 ± 24 | (78 ± 28) ×10$^3$ |
| Chitlac-THICK | 156 ± 44 | n = 36 | (106 ± 48) ×10$^3$ | 101 ± 15 | (81 ± 18) ×10$^3$ |
| | n = number of slides | | | | |
| | Chitosan-THIN *vs.* Chitlac-THIN P = 0.67; Chitosan-THIN *vs.* Chitlac-THICK P = 0.13; Chitlac-THIN *vs.* Chitlac-THICK P = 0.06. | | Chitlac-THIN vs. Chitosan-THIN: P < 0.01 Chitlac-THICK vs. Chitosan-THIN: P < 0.001 Chitlac-THICK vs. Chitlac-THIN P = 0.53 | Chitlac-THIN vs Chitosan-THIN P = 0.08 Chitlac-THICK vs. Chitosan-THIN P = 0.51; Chitlac-THICK vs. Chitlac-THIN P = 0.29 | Chitlac-THIN vs Chitosan-THIN P < 0.01 Chitlac-THICK vs. Chitosan-THIN P < 0.001; Chitlac-THICK vs. Chitlac-THIN P = 0.73 |

By quantifying the total β-Tubulin III-positive area (μm$^2$) [40] detected in each field, we found that this value was significantly higher in the two Chitlac-based substrates (see Table 1B).

This observation suggests that Chitlac-based substrates improved neuronal growth, leading to hippocampal neurons displaying wider outgrowth of neuronal processes,

since the total number of neurons was unchanged. Similarly, such substrates did not affect the number of GFAP positive glial cells that showed comparable values in cells/mm$^2$ (see Table 1C).

However, in a similar way GFAP positive areas progressively increased when measured from Chitosan-THIN to Chitlac-THICK (see Table 1D).

In the three substrates where neurons were detected, we performed single-cell patch-clamp recordings. We first assessed neuronal passive membrane properties. Membrane capacitance, $C_m$, values increased from Chitosan-THIN to Chitlac-THICK matrices (see Table 2A) while the opposite happened for input resistance, $R_{in}$, values (see Table 2B). This is in accordance with the suggestion that Chitlac facilitates neuronal dendritic tree formation.

**Table 2**. Electrophysiological recordings.

| | **A** | | **B** | **C** | | **D** | **E** | **F** |
|---|---|---|---|---|---|---|---|---|
| **SUBSTRATES** | single cell patch clamp | | | voltage clamp - spontaneous post-synaptic currents (PSCs) | | | PSCs in the presence of tetrodotoxin (TTX, 1μM) | |
| | membrane capacitance, $C_m$ | | input resistance, $R_{in}$ | PSCs frequency | | PSCs peak amplitude | mPSCs frequency | mPSCs peak amplitude |
| | *pF* | | *MΩ* | *Hz* | | *pA* | *Hz* | *pA* |
| Chitosan-THIN | 40.7 ± 14.6 | n = 73 | (1.1 ± 0.7) $\times 10^3$ | 1.6 ±1.5 | n = 64 | 38 ± 18 | 0.5 ± 0.4 n =13 | 15.7 ± 6.1 |
| Chitlac-THIN | 46.7 ± 17.2 | n = 102 | (0.9 ± 0.5) $\times 10^3$ | 2.2 ± 2.6 | n = 85 | 37 ± 15 | n.d. | n.d. |
| Chitlac-THICK | 49.3 ± 18.0 | n= 103 | (0.8 ± 0.5) $\times 10^3$ | 3.6 ± 3.1 | n = 96 | 51 ± 29 | 1.1 ± 1.0 n = 10 | 18.1 ± 6.3 |
| | Chitosan-THIN vs. Chitlac-THIN P < 0.05, Chitosan-THIN vs. Chitlac-THICK P < 0.01 Chitlac-THICK vs. Chitlac-THIN P = 0.26 | | Chitosan-THIN both vs. Chitlac-THIN and vs. Chitlac-THICK: P < 0.01 Chitlac-THICK vs. Chitlac-THIN P = 0.50 | Chitosan-THIN and Chitlac-THIN vs. Chitlac-THICK ***P < 0.001 Chitosan-THIN and Chitlac-THIN: P = 0.13 | | Chitosan-THIN and Chitlac-THIN vs. Chitlac-THICK: P < 0.001 Chitosan-THIN and Chitlac-THIN: P = 0.95 | Chitosan-THIN vs. Chitlac-THICK: P < 0.05 | Chitosan-THIN vs. Chitlac-THICK: P = 0.38 |

Under voltage clamp recordings, we measured the occurrence of spontaneous post-synaptic currents (PSCs; Figure 2B). The appearance of these heterogeneous events provides a clear evidence of functional synapse formation and network efficacy [28,45]. Box plots in Figure 2C and 2D summarize the values of PSCs frequency and PSCs peak amplitude; numerical data are reported in Table 2, C and D, respectively. Both values significantly increased in neurons grown on Chitlac-THICK when compared with the other growth substrates. No significant differences were present between Chitosan-THIN and Chitlac-THIN. Neurons on Chitlac-THICK thus showed an increased growth and an improved spontaneous synaptic activity.

To ascertain whether an improved synaptogenesis accompanied these observations, we focused our next experiments on this substrate as compared with Chitosan-THIN. We recorded PSCs in the presence of tetrodotoxin (TTX, 1μM), a voltage-gated $Na^+$ channel blocker that inhibits action potential (AP) generation. The events recorded in these conditions, called miniature PSCs (mPSCs; see sample tracings in Figure 2E), are AP-independent and rely on the stochastic fusion of neurotransmitter vesicles at the presynaptic membrane. Their frequency is proportional to the number of synaptic contacts [46]. We detected an increment in the mPSCs frequency in neurons grown on Chitlac-THICK with respect to neurons cultured on Chitosan-THIN thin layer (results summarized in Figure 2F), while mPSCs amplitudes were not affected (see Table 2E, F).

This first set of neurophysiology experiments strongly indicates that among the different polysaccharides and configurations tested, Chitlac-THICK is the best performer in favoring neuronal growth and synapse formation.

**3.3. Effect of polysaccharide-coated surfaces on fetal neural progenitor cells**

In the next set of experiments, we interfaced a class of stem cells isolated from the rat brain, the fetal neural progenitor cells (fNPCs), to the three different substrates to investigate whether fNPC behavior was also variably controlled by the three biomaterials. fNPCs at 2 weeks *in vitro* (WIV) adhered to all substrates and differentiated into glial and neuronal lineages, as shown in Figure 3A (visualizing β-Tubulin III-positive neurons and GFAP-positive astrocytes). By quantifying the total number of cells (by DAPI nuclei labeling, that is, including non-differentiated fNPCs), we observed that this value was significantly lower on Chitlac-THICK when compared with Chitosan-THIN (see Table 3A).

**Table 3**. Effect of polysaccharide-coated surfaces on differentiation efficiency of fNPC

| | *fetal neural progenitor cells (fNPC)* | | | | | | |
|---|---|---|---|---|---|---|---|
| **SUBSTRATES** | **A** | | **B** | | **C** | **D** | |
| | total number of cells | | β-Tubulin III-positive area | | GFAP-positive area | β-Tubulin III-positive area, positive for MAP2 | |
| | *cells/mm²* | | *μm²* | | | | |
| Chitosan-THIN | 549 ± 312 | n = 50 | 11± 10 | n = 25 | 29 ± 14 | 57 ± 14 | n = 12 |
| Chitlac-THIN | 447 ± 296 | n = 72 | 9 ± 7 | n = 26 | 29 ± 18 | 60 ± 20 | n = 11 |
| Chitlac-THICK | 402 ± 325 | n = 54 | 7 ± 6 | n = 21 | 17 ± 12 | 71 ± 14 | n = 11 |
| | Chitlac-THIN vs. Chitosan-THIN P = 0.07. Chitlac-THIN vs. Chitlac-THICK P = 0.42 Chitosan-THIN vs. Chitlac-THICK P < 0.05 | | Chitlac-THIN vs. Chitosan-THIN P = 0.41. Chitlac-THIN vs. Chitlac-THICK P = 0.29 Chitosan-THIN vs. Chitlac-THICK P = 0.07 | | Chitosan-THIN and Chitlac-THIN vs. Chitlac-THICK P < 0.05 Chitosan-THIN vs. Chitlac-THIN P = 0.99 | Chitosan-THIN vs. Chitlac-THICK P < 0.05 Chitosan-THIN vs. Chitlac-THIN P = 0.67 Chitlac-THICK vs. Chitlac-THIN P = 0.12 | |

**Table 4**. Effect of polysaccharide-coated surfaces on differentiation efficiency of MN progenitors in co-culture with neurotrophins-producing MABs.

| | *Motor neuron progenitors in co-colture with neurotrophins-producing MABs* | | | | | | |
|---|---|---|---|---|---|---|---|
| **SUBSTRATES** | **A** | **B** | | | **C** | | |
| | β-Tubulin III + GFAP+ cells/total number of cells | β-Tubulin III-positive area | | | % of ChAT positive cells/number of β-Tubulin III-positive neurons | | |
| | F10 (MABs-NGF) | D16 (control - MABs) | A9 (MABs-BDNF) | F10 (MABs-NGF) | D16 (control MABs) | A9 (MABs-BDNF) | F10 (MABs-NGF) |
| | *%* | *$\mu m^2$* | | | *%* | | |
| Chitosan-THIN | 48 ± 5 | $(31 \pm 12)\times10^3$ | $(33\pm 11)\times10^3$ | $(32+12)\times10^3$ | 21 ± 7 n=10 | 41 ± 8 n=10 | 33 ± 7 n=10 |
| Chitlac-THIN | 65 ± 12 | $(33\pm 12)\times10^3$ | $(36\pm 14)\times10^3$ | $(42\pm 14)\times10^3$ | 27 ± 6 n=10 | 40 ± 11 n=10 | 60 ± 7 n=10 |
| Chitlac-THICK | 75 ± 8 | $(37\pm 16)\times10^3$ | $(51\pm 15)\times10^3$ | $(62\pm 12)\times10^3$ | 80 ± 8 n=10 | 82 ± 7 n=10 | 93 ± 5 n=10 |
| | Chitosan-THIN vs. Chitlac-THIN $P < 0.01$, Chitosan-THIN vs. Chitlac-THICK $P < 0.01$<br><br>n = 5 total fields | Chitosan-THIN and Chitlac-THIN vs. Chitlac-THICK $P < 0.01$ Chitosan-THIN vs. Chitlac THIN P= 0.3<br><br>n= 5 total fields | Chitosan-THIN and Chitlac-THIN vs. Chitlac-THICK $P < 0.01$ Chitosan-THIN vs. Chitlac THIN P= 0.09<br><br>n= 5 total fields | Chitosan-THIN and Chitlac-THIN vs. Chitlac-THICK $P < 0.01$ Chitosan-THIN vs. Chitlac THIN $P < 0.01$<br><br>n= 5 total fields | Chitosan-THIN and Chitlac-THIN vs. Chitlac-THICK $P < 0.01$ Chitosan-THIN vs. Chitlac THIN P= 0.7<br><br>n= 10 total fields | Chitosan-THIN and Chitlac-THIN vs. Chitlac-THICK $P < 0.01$ Chitosan-THIN vs. Chitlac THIN P= 0.6<br><br>n= 10 total fields | Chitosan-THIN vs. Chitlac-THIN and vs Chitlac THICK $P < 0.001$<br>Chitlac-THIN vs. Chitlac-THICK $P < 0.01$<br><br>n= 10 total fields |

We then computed the amount of GFAP-positive area and that of β-Tubulin III-positive one (expressed as % of each sampled field, plot in Figure 3C). The latter computed ratio was not statistically different between the three substrates (see Table 3 B). At variance, the GFAP-positive ratio was lower on Chitlac-THICK with respect to the other two materials (see Table 3C). Thus, regarding the total amount of fNPCs that adhered and grew on the different platforms, the Chitlac-THICK one seemed to favor the neuronal lineage growth.

To test whether neuronal maturation was also improved in this condition, we measured the amount of β-Tubulin III-positive area that was also positive for the mature neuronal marker MAP2 ([47]; as % of double-positive cells in the plot of Figure 3D). This value was significantly increased in Chitlac-THICK when compared with Chitosan-THIN (see Table 3D). This finding indicates that progenitor cells that had differentiated into neurons acquired, at the time tested, a higher degree of maturation on Chitlac (and particularly so on Chitlac-THICK) coating.

**3.4. Effect of polysaccharide-coated surfaces on motor neuron progenitors**

To further compare the efficacy of the new biocompatible growth platforms under scrutiny in promoting stem cell differentiation into motor neurons we generated more sophisticated bioconstructs, where we co-cultured E2GFP-D7 cells with control- or neurotrophin-producing mesoangioblasts (MABs). E2GFP-D7 cells (D7) are motor neuron (MN) progenitors that derive from a transgenic mouse line for a specific enhancer (E2-Ngn2) of the pro-neural gene Neurogenin2 (Ngn2), which plays an important role in MN generation and development [48-49]. As E2-Ngn2 enhancer is specifically active only in spinal MN progenitors, this cell line provides a selected source of pure MN progenitors that can be efficiently differentiated *in vitro* into MN. We thus used clone D7 cells in order to evaluate the impact of the three different

substrates on MN differentiation. In addition, since motor neurons differentiation is usually controlled by nerve growth factor (NGF) and/or by brain-derived neurotrophic factor (BDNF), we co-cultured D7 progenitors with control (clone D16-MAB) or neurotrophin producing-MABs. These mesenchymal stem cells, due to their high and adhesion-dependent migratory capacity, hold the potential, *in vivo*, to reach perivascular targets especially in damaged areas [50], with an obvious impact in the exploitation of cell replacement strategies. We used genetically modified MABs constitutively expressing GFP (namely clone D16) [51], and MABs additionally producing NGF (MABs-NGF, clone F10) or BDNF (MABs-BDNF, clone A9). Both F10 and A9 cells ensure a continuous and concentrated localized supplementation of neurotrophic factors [37], but were never tested in complex bio-constructs or interfaced with various biomaterials. MABs equally grew on Chitosan-THIN, Chitlac-THIN and Chitlac-THICK surfaces (Figure S2, Supporting Information). We next co-cultured, on the different substrates, D7 progenitors combined with the three types of MABs. Figure 4A shows D7 differentiation in the three different co-cultures grown on the three bio-substrates, giving rise to both β-Tubulin III-positive neurons and GFAP-positive astrocytes.

The differentiation efficiency was quantified as β-Tubulin III + GFAP positive cells/ total number of cells (Figure 4B). Interestingly, the highest efficiency, in the presence of NGF-producing MABs (F10, right panel), was reached when D7 progenitors differentiated on Chitlac-THICK substrate (bottom-right panel; D7/F10; see Table 4A, B). Moreover, the β-Tubulin III-positive neurons displayed an increased neural arborization when cultured on this substrate and in the presence of neurotrophic factors, suggestive of higher degree of neuronal maturation (β-Tubulin III-positive area reported in $\mu m^2$: see Table 4B). To strengthen this result, we measured the

Choline Acetyltransferase- (ChAT) positive cells (Figure 4D), to estimate the number of differentiated cholinergic neurons, namely MN [52]. We detected more ChAT-positive MNs when D7 progenitors differentiated in the presence of MABs - and particularly so with MABs-NGF (F10) - on Chitlac-THICK compared with the other substrates. The results are summarized by the plot in Figure 4C, as % of ChAT positive cells/number of β-Tubulin III-positive neurons; numerical results are reported in the three columns of Table 4 C, for the different clone combinations considered.

Altogether, this data strongly support Chitlac-THICK substrate as an ideal biomaterial particularly suited to implement growth and differentiation of neuronal and MN progenitors.

**3.5. Engineering local release of neurotrophins shapes synaptic network formation on Chitlac-THICK platforms**

Finally, we explored the idea of generating cellularized bio-constructs that can be tailored towards combined treatments in CNS engineering strategies. We used the continuous release of growth factors brought about by neurotrophins producing-MABs combined with the most promising substrate favoring neuronal growth (Chitlac-THICK) to shape synaptic network formation in primary neuronal cultures. To this aim, we co-cultured (for the first time ever to the best of our knowledge) dissociated hippocampal neurons with control and neurotrophins producing-MABs on the Chitlac-THICK substrate. Neurons grew readily on all four conditions (Figure 5A) with comparable neuronal densities (see Table 5A).

**Table 5**. Local release of neurotrophins and synaptic network formation on Chitlac-THICK.

| *Dissociated hippocampal neurons on Chitlac-THICK platforms in the presence of neurotrophins producing-MABs* | | | | | | | |
|---|---|---|---|---|---|---|---|
| | | Cellular growth | | | spontaneous post-synaptic currents (PSCs) | | |
| **CELL TYPES** | | **A** | | **B** | **C** | | **D** |
| | | neuronal density | | β-Tubulin III-positive area | PSCs frequency | | PSCs peak amplitude |
| | | *neurons/mm$^2$* | | *$\mu m^2$* | *Hz* | | *pA* |
| (Co-)cultures | Control | 162 ± 95 | n = 16 | (107 ± 27) × $10^3$ | 2.8 ± 2.9 | n = 14 | 48 ± 20 |
| | D 16 | 154 ± 91 | n = 19 | (147 ± 47) × $10^3$ | 2.7 ± 2.2 | n = 20 | 68 ± 29 |
| | A9 | 144 ± 74 | n = 28 | (139 ± 45) × $10^3$ | 5.6 ± 4.4 | n = 16 | 64 ± 18 |
| | F10 | 127 ± 87 | n = 21 | (184 ± 77) × $10^3$ | 6.2 ± 5.0 | n = 17 | 81 ± 32 |
| Control = dissociated hippocampal cultures alone;<br>D16 = co-culture with control MABs;<br>A9 = co-culture with BDNF-producing MABs;<br>F10 = co-culture with NGF-producing MABs. | | Control vs. D16 P = 0.79,<br>vs. A9 P = 0.49,<br>vs. F10 P = 0.22;<br>D16 vs. A9 P = 0.67,<br>vs. F10 P = 0.32;<br>A9 vs. F10 P = 0.51 | | Control vs. F10 P < 0.001,<br>D16 vs. F10 P < 0.05,<br>A9 vs. F10 P<0.01,<br>Control vs. D16 P = 0.06,<br>vs. A9 P = 0.11,<br>D16 vs. A9 P = 0.65 | Control vs. A9 and F10 P < 0.05,<br>D16 vs. A9 P < 0.05,<br>vs. F10 P < 0.01,<br>Control vs. D16 P = 0.94,<br>A9 vs. F10 P = 0.62 | | Control vs. D16 and A9 P < 0.05,<br>Control vs. F10 P < 0.001,<br>D16 vs. A9 P = 0.66,<br>vs. F10 P = 0.14,<br>A9 vs. F10 P = 0.07 |

However, estimating neuronal dendrites outgrowth by β-Tubulin III-positive area ($\mu m^2$) revealed a significantly larger network of neuronal processes in F10-MABs NGF compared with the other combinations (see Table 5B).

When recording spontaneous synaptic activity, PSCs (Figure 5B), we noticed that both PSCs frequency (Box plot in Figure 5C and Table 5 C) and peak amplitude (Box Plots in Figure 5D and Table 5D) were further boosted by the presence of the neurotrophins.

To note, PSC peak amplitude values also increased when primary neurons were co-cultured with control MABs, suggesting that MABs *per se* were able to interfere with the neuronal network formation. Taken together, our results show that the improvement of the synaptic activity driven by the Chitlac-THICK substrate can be tuned by the additional inclusion of MAB reservoir of neurotrophins such as BDNF and NGF.

## 4. Discussion

The results presented here provide new knowledge for the design of polysaccharide-based composites for nerve tissue engineering. We have shown that a coating consisting of Chitlac, enriched through the exploitation of electrostatic interactions of the - otherwise biologically inert - polyanion Alginate, favor postnatal neurons growth, synapse formation and the differentiation of stem cells into the proper neuronal lineage. We have further shown that sophisticated bio-constructs enriched with MABs, engineered to provide local delivery of growth factors, were indeed well supported by this material.

*The bio-construct: the materials*

The surface regularity and thickness reproducibility of the polysaccharide coatings, reported by confocal and AFM measurements, relayed on the electrostatic interactions between the polysaccharides and the glass surface [53]. Glass coverslips were in fact

activated by piranha solution, introducing negative charges, exploited to establish the interactions between the glass surface and the amino groups of Chitlac and Chitosan. A similar approach, based on the electrostatic interactions between the cationic polysaccharide Chitlac and (anionically) activated surfaces, was successfully employed for the methacrylate-based material functionalization to adsorb Chitlac on thermosets [4,25] or entangle it within Alginate-based tridimensional scaffolds [17]. The amount of Chitlac adsorbed onto the anionized glass surface is always lower than that of Chitosan. This can likely be ascribed to the (much) lower (positive) charges brought by Chitlac with respect to Chitosan, given the lower $pK_a$ values of the secondary amines in Chitlac with respect to the primary ones [43]. Electrostatic interactions are also at the root of the effective use of Alginate polyanion to increase the amount of adsorbed polycations: the relative increase of thickness is +105% and +380% for Chitosan and Chitlac, respectively.

We reported differences in the material surface properties, (by studying their free energy parameters), including hydrophilicity, wettability and charge, all these being key mechanisms in driving protein absorption, and thus, crucial in guiding biological responses once cells are exposed to the materials within living organisms [54]. By contact angle analysis Chitlac showed higher wettability and hydrophilicity when compared with Chitosan, probably due to its chemical structure, in accordance with recent findings [43], that showed how the glucitol-galactose (lactitol) side-groups of Chitlac determine a stronger interaction with water (solvation zone) with respect to Chitosan.

To shed light on the interactions taking place on the polysaccharide-coated surfaces we calculated their surface energies expressed as a sum of the dispersive (LW) and acid-base (AB) contribution, namely taking into account both non-polar and polar interactions, respectively [24]. The total surface energy was in line with previous investigations on polysaccharide-coated methacrylate-based surfaces [25]. From the

contact angle data for polar liquids, the acid−base work of adhesion $W^{AB}$ was calculated for the different coated surfaces. Including Chitlac in the biomaterials lead to a significant increase of acid−base interactions with water, which reflected higher density of polar functional groups of Chitlac. This result can be traced back the different chemical structure of the macromolecules adsorbed on the surface, *i.e.* the presence of the lactose residues in the case of Chitlac, which determines a higher density of surface hydroxyl sites. These observations strengthen the notion that surface energy parameters and interfacial interactions of polar liquids provide a reasonable description of the acid−base character of the polysaccharide-based surfaces. Conversely, the dispersive interactions did not vary between Chitlac or Chitosan containing surfaces, in accordance with previous reports [3, 55-56], on surfaces coated with different polymers or treated with different procedures. It has been recently reported that the arrangement of polar and non-polar groups at the nanoscale is crucial in generating surface energy gradients that are sensed by cell lines, such as PC12 [3]. It is tempting to speculate that surface free-energy gradients bear a critical impact on the relevant biological processes - including CNS regeneration - supported and favored by biomaterials.

*The bio-construct: post-natal neurons*

The use of polysaccharides for tissue engineering requires the design, synthesis and characterization of polysaccharide-based bioactive structures for promoting new tissue in-growth [57]. Alginate/(lactose-modified Chitosan) hydrogels have been engineered into biologically active 3D scaffolds that promoted chondrocyte growth and proliferation [19]. In nerve tissue engineering, Chitosan biomaterials, decorated with trophic factors and combined with stem cells, were used to reconstruct a positive microenvironment favoring spinal cord regeneration after experimental injury [14]. For a further development of the use of these materials for effective neuronal adhesion, growth and differentiated cell function, we demonstrated incremental

positive effects of Chitlac. In order to increase the very thin layer obtained on glass coverslips, which might limit its interaction with cells, additional electrostatic interactions through Alginate, an inert anionic polysaccharide, were exploited. This thicker coating, indicated as Chitlac-THICK, when compared with Chitlac or Chitosan thin layers, represented the most promising composite. This is apparently unrelated to mere differences in homogeneity of the various composite distributions on the growth interfaces. Much in the same way, we cannot specifically ascribe the neuronal nor the progenitors' increased ability to grow and differentiate to the hydrophilic properties of Chitlac-THICK only, nor to its surface free energy and work of adhesion parameters, which did not differ from Chitlac in the thin layer. Indeed, we can only put forward a combination between the more favorable surface conditions for protein adsorption already brought about by Chitlac in the thin layer - when compared with Chitosan-THIN and the Chitlac-THICK larger thickness. The latter parameter (obviously enormously enhanced by the very high water uptake by Chitlac [43] in the hydrated conditions of the biological experiment) likely provides a much less constrained physical-chemical environment adequate to neuronal development. Thus, the *neuro-favorable* environment could also be due to the direct recreation of ECM-like microenvironment by Chitlac and the improved physical microenvironment, leading to the deposition of an ECM-mimic, more permissive for synapse construction [58]. In Chitlac-THICK neuronal networks, an improved connectivity always accompanies the increased neuronal growth (as suggested by the larger β-Tubulin III-positive area). In Chitlac-THICK coatings, we measured an increase in PSC frequency, without reporting changes in the network size [29]. In fact, the neuronal densities were similar, when compared with the other growth substrates, as shown by our immunocytochemistry experiments. In accordance with the data concerning spontaneous PSCs, we recorded an increase in the frequency of mPSC in neurons grown on Chitlac-THICK carpets. mPSC frequency is a widely accepted

index of the number of active zones or of synaptic contacts at presynaptic terminals, while mPSC amplitude is connected with the amount of neurotransmitter receptors expressed at the postsynaptic membrane [46]. Therefore, the improvement in the detected neural network activity seemed to be mainly related to modifications occurring at the presynaptic level, a hypothesis strengthened by the larger neuronal growth reported by immunocytochemistry experiments. The different geometries of hippocampal cells on the diverse substrates were also of interest: the low incidence of clustered cells on Chitlac-THICK material supports the higher biocompatibility of the substrate or a more even distribution of adhesion proteins.

*The bio-construct: progenitor stem cells*

Confirming the Chitlac-THICK affinity for the neuronal phenotypes, also fNPCs differentiated better on these substrates. To note, we also tested a combination of embryonic spinal cord progenitors, as source of motor neurons, and engineered mesoangioblasts, as source of NGF or BDNF. The advantages of this combinatorial approach are manifold. On one hand, the E2D7 cells are able to give rise to fully differentiated MNs, but retain at the same time the ability to generate astrocytes and oligodendrocytes. On the other hand, these progenitors do not pose the drawback to induce tumor formation when transplanted *in vivo*, as other type of stem cells (*i.e.* ESCs, iPSCs) might do [59-60]. In addition, the continuous release of NGF or BDNF from MABs greatly increases the overall differentiation of E2D7 progenitors: it was further improved in the Chitlac-THICK microenvironment. Neurotrophins play a pivotal role in sustaining neuronal differentiation, exerting neuroprotective function and inducing MN differentiation [61]. Interestingly, both BDNF and NGF, together with another neurotrophin, NT-3, have been found to be up regulated in injured spinal cord upon stem cells transplantation [62]. Among the different neurotrophins, BDNF is considered one of the more effective in driving motor neuron differentiation. Unexpectedly, we obtained more ChAT-positive motor neurons when E2GFP

progenitors were exposed to NGF with respect to BDNF. We cannot exclude that this particular cellular model is more responsive to NGF, when neuronal differentiation is tested. Alternatively, we may suggest that, due to the cholinergic phenotype, these motor neurons particularly benefit, during their differentiation, from being exposed to NGF, as known for other cholinergic neurons [63]. Intriguingly, recent microarray gene profiling of E2GFP progenitors reported high level of expression of neuritin 1 (Scardigli, unpublished data), an NGF effector involved in motor neuron growth and neuro-muscolar synaptogenesis [64-66]. Ultimately, we have also to consider that other secreted molecules, not yet characterized, released from MABs, may provide, in synergy with NGF, rather than with BDNF, a more favorable milieu for motor differentiation of E2GFP progenitors. NGF has been widely used in combination with different biomaterials (heparin-based hydrogel, gelatin lipid carriers, Chitosan microspheres) in therapeutic approaches for spinal cord injury treatment in animal models, showing an improvement in inducing neuronal functions [67-69]. More recently, Yang *et al.* demonstrated that the combination of Chitosan and NT-3 as implantable scaffold was able to induce local neurogenesis *in vivo* after spinal injury [14]. At variance with these approaches - where the neurotrophic factors need to be loaded on the scaffold at limited and fixed concentration - the novelty of our study is to use MABs as source of a continuous and localized release of NGF and BDNF. This allows for a constant supply of bioactive neurotrophins to the MN progenitors present in the Chitlac-THICK structure, which we demonstrated to be more effective than Chitosan in promoting neuronal growth. Our experiments further confirmed the efficacy of MABs in promoting neuronal network growth and activity, since Chitlac-THICK surface supported the growth of post-natal neurons in the presence of non-releasing, NGF-releasing or BDNF-releasing MABs.

## 5. Conclusions

Chitlac-THICK substrates are able to promote neuronal growth, differentiation, maturation and formation of synapses. These observations support this new material as a promising candidate for the development of complex bio-constructs promoting CNS regeneration. This is, to our knowledge, the first time in which Chitlac composites have been tested in the CNS. Chitlac affinity for neurons might be related to its chemical nature and to the differences in surface energies between Chitlac and Chitosan. The presence of a large amount of lactitol branches on the Chitosan backbone caused a considerable increase of surface hydrophilicity, polarity and acid-base work of adhesion. Moreover but not surprisingly, the expedient use of Alginate to increase the thickness of the polycation coating was a successful strategy only with Chitlac but not with Chitosan because only the former derivative is miscible with the algal polyanion. At variance with Chitosan, the Chitlac/Alginate system can be described as an interpenetrated polymer network in solution, with high viscosity but fully permeable by solutes, biological macromolecules and favorable to the embedding and growth of cells.

Additional experimental evidence will be necessary to clarify whether the enhanced differentiation of neurons on Chitlac-based substrates can be ascribed solely to the combined effect of the more hydrophilic and polar layer or also to some biological activity of the polysaccharide. Future work will be focused also on the development of three-dimensional biomaterials based on alginate and Chitlac (hydrogels or porous scaffold) in order to evaluate the effects of the three-dimensional environment *in vitro* and to explore the possibility of an *in vivo* application of these polysaccharides. Our novel findings sustain the exploitation of polysaccharide-based scaffolds able to favor neuronal network reconstruction. The development of hybrid cell-material bio-construct holds the potential to improve our knowledge on the surface interactions that neurons are able to probe and to which to respond.

**Acknowledgements**

We acknowledge financial support from the NEUROSCAFFOLDS-FP7-NMP-604263 and PRIN-MIUR n. 2012MYESZW. M. Pulin is kindly acknowledged for contributing to the firsts set of Chitlac testing.

**Competing interest statement**

We declare no competing interest.

**References**

[1] D. Drago, C. Cossetti, N. Iraci, E. Gaude, G. Musco, A. Bachi, S. Pluchino, The stem cell secretome and its role in brain repair, Biochimie. 95 (2013) 2271-2285.

[2] J.M. Soria, R.C. Martinez, O. Bahamonde, D.M. Garcia Cruz, S.M. Salmeron, M.A. Garcia Esparza, C. Casas, M. Guzmán, X. Navarro, J.L. Gómez Ribelles, J.M. García Verdugo, M. Monleón Pradas, J.A. Barcia, Influence of the substrate's hydrophilicity on the in vitro Schwann cells viability, J. Biomed. Mater. Res. A 83 (2007) 463-470.

[3] G. Lamour, A. Eftekhari-Bafrooei, E. Borguet, S. Soues, A. Hamraoui, Neuronal adhesion and differentiation driven by nanoscale surface free-energy gradients, Biomaterials 31 (2010) 3762-3771.

[4] A. Travan, I. Donati, E. Marsich, F. Bellomo, S. Achanta, M. Toppazzini, S. Semeraro, T. Scarpa, V. Spreafico, S. Paoletti, Surface modification and polysaccharide deposition on BisGMA/TEGDMA thermoset, Biomacromolecules 11 (2010) 583-592.

[5] T. Boudou, T. Crouzier, K. Ren, G. Blin, C. Picart, Multiple functionalities of polyelectrolyte multilayer films: new biomedical applications, Adv. Mater. 22 (2010) 441-467.

[6] E. Marsich, A. Travan, I. Donati, G. Turco, J. Kulkova, N. Moritz, H.T. Aro, M. Crosera, S. Paoletti, Biological responses of silver-coated thermosets: an in vitro and in vivo study, Acta Biomater. 9 (2013a) 5088-5099.

[7] R. Jayakumar, D. Menon, K. Manzoor, S.V. Nair, H. Tamura, Biomedical applications of chitin and Chitosan based nanomaterials-A short review, Carbohydr. Polym. 82 (2010) 227-232.

[8] Z. Wei, J. Zhao, Y.M. Chen, P. Zhang, Q. Zhang, Self-healing polysaccharide-based hydrogels as injectable carriers for neural stem cells, Sci. Rep. 6 (2016) 37841.

[9] Q. Gu, E. Tomaskovic-Crook, R. Lozano, Y. Chen, R.M. Kapsa, Q. Zhou, G.G. Wallace, J.M. Crook, Functional 3D Neural Mini-Tissues from Printed Gel-Based Bioink and Human Neural Stem Cells, Adv. Healthc. Mater. 5 (2016) 1429-1438.

[10] C.A. McKay, R.D. Pomrenke, J.S. McLane, N.J. Schaub, E.K. DeSimone, L.A. Ligon, R.J. Gilbert, An injectable, calcium responsive composite hydrogel for the treatment of acute spinal cord injury, ACS Appl. Mater. Interface 6 (2014) 1424-1438.

[11] J. Du, E. Tan, H.J. Kim, A. Zhang, R. Bhattacharya, K.J. Yarema, Comparative evaluation of chitosan, cellulose acetate, and polyethersulfone nanofiber scaffolds for neural differentiation, Carbohydr. Polym. 99 (2014) 483-490.

[12] N.L. Francis, P.M. Hunger, A.E. Donius, B.W. Riblett, A. Zavaliangos, U.G. Wegst, M.A. Wheatley, An ice-templated, linearly aligned chitosan-alginate scaffold for neural tissue engineering, J. Biomed. Mater. Res. A 101 (2013) 3493-3503.

[13] R. Jian, Y. Yixu, L. Sheyu, S. Jianhong, Y. Yaohua, S. Xing, H. Qingfeng, L. Xiaojian, Z. Lei, Z. Yan, X. Fangling, G. Huasong, G. Yilu, Repair of spinal cord injury by chitosan scaffold with glioma ECM and SB216763 implantation in adult rats, J. Biomed. Mater. Res. A 103 (2015) 3259-3272.

[14] Z. Yang, A. Zhang, H. Duan, S. Zhang, P. Hao, K. Ye, Y.E. Sun, X. Li, NT3-Chitosan elicits robust endogenous neurogenesis to enable functional recovery after spinal cord injury, PNAS 112 (2015) 13354-13359.

[15] H. Li, A.M. Koenig, P. Sloan, N.D. Leipzig, In vivo assessment of guided neural stem cell differentiation in growth factor immobilized chitosan-based hydrogel scaffolds, Biomaterials 35 (2014) 9049-9057.

[16] P. Marcon, E. Marsich, A. Vetere, P. Mozetic, C. Campa, I. Donati, F. Vittur, A. Gamini, S. Paoletti, The role of Galectin-1 in the interaction between chondrocytes and a lactose-modified Chitosan, Biomaterials 26 (2005) 4975-4984.

[17] E. Marsich, F. Bellomo, G. Turco, A. Travan, I. Donati, S. Paoletti, Nano-composite scaffolds for bone tissue engineering containing silver nanoparticles: preparation, characterization and biological properties, J. Mater. Sci. Mater. Med. 24 (2013b) 1799-1807.

[18] E. Marsich, A. Travan, M. Feresini, R. Lapasin, S. Paoletti, I. Donati, Polysaccharide-based polyanion–polycation–polyanion ternary systems in the concentrated regime and hydrogel form, Macromol. Chem. Phys. 214 (2013c) 1309−1320.

[19] E. Marsich, M. Borgogna, I. Donati, P. Mozetic, B.L. Strand, S.G. Salvador, F. Vittur, S. Paoletti, Alginate/lactose-modified chitosan hydrogels: a bioactive biomaterial for chondrocyte encapsulation, J. Biomed. Mater. Res. A 84 (2008) 364-376.

[20] D. Porrelli, A. Travan, G. Turco, E. Marsich, M. Borgogna, S. Paoletti, I. Donati, Alginate–hydroxyapatite bone scaffolds with isotropic or anisotropic pore structure: material properties and biological behavior, Macromol. Mater. Eng. 300 (2015) 989-1000.

[21] I. Donati, S. Stredanska, G. Silvestrini, A. Vetere, P. Marcon, E. Marsich, P. Mozetic, A. Gamini, S. Paoletti, F. Vittur, The aggregation of pig articular chondrocyte and synthesis of extracellular matrix by a lactose-modified Chitosan, Biomaterials 26 (2005) 987-998.

[22] D. Nečas, P. Klapetek, Gwyddion: an open-source software for SPM data analysis, Cent. Eur. J. Phys. 10 (2012) 181-188.

[23] D.Y. Kwok, A.W. Neumann, Contact angle measurement and contact angle interpretation, Adv. Colloid Interface Sci. 81 (1999) 167-249.

[24] C.J. Van Oss, M.K. Chaudhury, R.J. Good, Interfacial Lifshitz-van der Waals and polar interactions in macroscopic systems, Chem. Rev. 88 (1988) 927-941.

[25] A. Travan, E. Marsich, I. Donati, M.P. Foulc, N. Moritz, H.T. Aro, S. Paoletti, Polysaccharide-coated thermosets for orthopedic applications: from material characterization to in vivo tests, Biomacromolecules 13 (2012) 1564-1572.

[26] V. Lovat, D. Pantarotto, L. Lagostena, B. Cacciari, M. Grandolfo, M. Righi, G. Spalluto, M. Prato, L. Ballerini, Carbon nanotube substrates boost neuronal electrical signaling, Nano Lett. 5 (2005) 1107-1110.

[27] G. Cellot, E. Cilia, S. Cipollone, V. Rancic, A. Sucapane, S. Giordani, L. Gambazzi, H. Markram, M. Grandolfo, D. Scaini, F. Gelain, L. Casalis, M. Prato, M. Giugliano, L. Ballerini, Carbon nanotubes might improve neuronal performance by favouring electrical shortcuts, Nat. Nanotechnol. 4 (2009) 126-133.

[28] G. Cellot, F.M. Toma, Z.K. Varley, J. Laishram, A. Villari, M. Quintana, S. Cipollone, M. Prato, L. Ballerini, Carbon nanotube scaffolds tune synaptic strength in cultured neural circuits: novel frontiers in nanomaterial-tissue interactions, J. Neurosci. 31 (2011) 12945-12953.

[29] S. Bosi, R. Rauti, J. Laishram, A. Turco, D. Lonardoni, T. Nieus, M. Prato, D. Scaini, L. Ballerini, From 2D to 3D: novel nanostructured scaffolds to investigate signalling in reconstructed neuronal networks, Sci. Rep. 5 (2015) 9562.

[30] Q. He, T. Zhang, Y. Yang, F. Ding, In vitro biocompatibility of chitosan-based materials to primary culture of hippocampal neurons, J. Mater. Sci.: Mater. Med. 20 (2009) 1457-1466.

[31] X. Li, Z. Yang, A. Zhang, T. Wang, W. Chen, Repair of thoracic spinal cord injury by chitosan tube implantation in adult rats, Biomaterials 30 (2009) 1121-1132.

[32] G. Cellot, P. Lagonegro, G. Tarabella, D. Scaini, F. Fabbri, S. Iannotta, M. Prato, G. Salviati, L. Ballerini, PEDOT:PSS interfaces support the development of neuronal synaptic networks with reduced neuroglia response in vitro, Front. Neurosci. 9 (2016) 521.

[33] N.P. Pampaloni, D. Scaini, F. Perissinotto, S. Bosi, M. Prato, L. Ballerini, Sculpting neurotransmission during synaptic development by 2D nanostructured interfaces, Nanomedicine (2017).

[34] E.R. Aurand, J.L. Wagner, R. Shandas, K.B. Bjugstad, Hydrogel formulation determines cell fate of fetal and adult neural progenitor cells, Stem Cell Res. 12 (2014) 11-23.

[35] R. Scardigli, P. Capelli, D. Vignone, R. Brandi, M. Ceci, F. La Regina, E. Piras, S. Cintoli, N. Berardi, S. Capsoni, A. Cattaneo, Neutralization of nerve growth factor impairs proliferation and differentiation of adult neural progenitors in the subventricular zone, Stem Cells 32 (2014) 2516-2528.

[36] M. Sampaolesi, Y. Torrente, A. Innocenzi, R. Tonlorenzi, G. D'Antona, M.A. Pellegrino, R. Barresi, N. Bresolin, M.G. De Angelis, K.P. Campbell, R. Bottinelli, G. Cossu, Cell therapy of alpha-sarcoglycan null dystrophic mice through intra-arterial delivery of mesoangioblasts, Science 301 (2003) 487-492.

[37] T. Su, R. Scardigli, L. Fasulo, B. Paradiso, M. Barbieri, A. Binaschi, R. Bovolenta, S. Zucchini, G. Cossu, A. Cattaneo, M. Simonato, Bystander effect on brain tissue of mesoangioblasts producing neurotrophins, Cell Transplant. 21 (2012) 1613-1627.

[38] M. Medelin, V. Rancic, G. Cellot, J. Laishram, P. Veeraraghavan, C. Rossi, L. Muzio, L. Sivilotti, L. Ballerini, Altered development in GABA co-release shapes glycinergic synaptic currents in cultured spinal slices of the SOD1(G93A) mouse model of amyotrophic lateral sclerosis, J. Physiol. 594 (2016) 3827-3840.

[39] J.D. Clements, J.M. Bekkers, Detection of spontaneous synaptic events with an optimally scaled template, Biophys. J. 73 (1997) 220-229.

[40] S. Usmani, E.R. Aurand, M. Medelin, A. Fabbro, D. Scaini, J. Laishram, F.B. Rosselli, A. Ansuini, D. Zoccolan, M. Scarselli, M. De Crescenzi, S. Bosi, M. Prato, L. Ballerini, 3D meshes of carbon nanotubes guide functional reconnection of segregated spinal explants, Sci. Adv. 2 (2016) e1600087.

[41] J. Schindelin, I. Arganda-Carreras, E. Frise, V. Kaynig, M. Longair, T. Pietzsch, S. Preibisch, C. Rueden, S. Saalfeld, B. Schmid, J.Y. Tinevez, D.J. White, V. Hartenstein, K. Eliceiri, P. Tomancak, A. Cardona, Fiji: an open-source platform for biological-image analysis, Nature Methods 9 (2012) 676-682.

[42] I. Donati, I.J. Haug, T. Scarpa, M. Borgogna, K.I. Draget, G. Skjåk-Braek, S. Paoletti, Synergistic effects in semidilute mixed solutions of alginate and lactose-modified Chitosan (Chitlac), Biomacromolecules 8 (2007) 957-962.

[43] N. D'Amelio, C. Esteban, A. Coslovi, L. Feruglio, F. Uggeri, M. Villegas, J. Benegas, S. Paoletti, I. Donati, Insight into the molecular properties of Chitlac, a Chitosan derivative for tissue engineering, J. Phys. Chem. B 117 (2013) 13578-13587.

[44] K.S. Straley, C.W. Foo, S.C. Heilshorn, Biomaterial design strategies for the treatment of spinal cord injuries, J. Neurotrauma 27 (2010) 1-19.

[45] M. Siebler, H. Köller, C.C. Stichel, H.W. Müller, H.J. Freund, Spontaneous activity and recurrent inhibition in cultured hippocampal networks, Synapse 14 (1993) 206-213.

[46] M. Raastad, J.F. Storm, P. Andersen, Putative single quantum and single fibre excitatory postsynaptic currents show similar amplitude range and variability in rat hippocampal slices, Eur. J. Neurosci. 4 (1992) 113-117.

[47] A. Harada, J. Teng, Y. Takei, K. Oguchi, N. Hirokawa, MAP2 is required for dendrite elongation, PKA anchoring in dendrites, and proper PKA signal transduction, J. Cell Biol. 158 (2002) 541-549.

[48] R. Scardigli, C. Schuurmans, G. Gradwohl, F. Guillemot, Crossregulation between Neurogenin2 and pathways specifying neuronal identity in the spinal cord, Neuron 31 (2001) 203-217.

[49] M.L. Liu, T. Zang, Y. Zou, J.C. Chang, J.R. Gibson, K.M. Huber, C.L. Zhang, Small molecules enable neurogenin 2 to efficiently convert human fibroblasts into cholinergic neurons, Nat. Commun. 4 (2013) 2183.

[50] B.G. Galvez, M. Sampaolesi, S. Brunelli, D. Covarello, M. Gavina, B. Rossi, G. Constantin, G. Torrente Cossu, Complete repair of dystrophic skeletal muscle by mesoangioblasts with enhanced migration ability, J. Cell Biol. 174 (2006) 231–243.

[51] S. Brunelli, E. Tagliafico, F.G. De Angelis, R. Tonlorenzi, S. Baesso, S. Ferrari, M. Niinobe, K. Yoshikawa, R.J. Schwartz, I. Bozzoni, S. Ferrari, G. Cossu, Msx2 and necdin combined activities are required for smooth muscle differentiation in mesoangioblast stem cells, Circ. Res. 94 (2004) 1571-1578.

[52] M.E. Hester, M.J. Murtha, S. Song, M. Rao, C.J. Miranda, K. Meyer, J. Tian, G. Boulting, D.V. Schaffer, M.X. Zhu, S.L. Pfaff, F.H. Gage, B.K. Kaspar, Rapid and efficient generation of functional motor neurons from human pluripotent

stem cells using gene delivered transcription factor codes, Mol. Ther. 19 (2011) 1905-1912.

[53] T. Haque, H. Chen, W. Ouyang, C. Martoni, B. Lawuyi, A.M. Urbanska, S. Prakash, Superior Cell Delivery Features of Poly(ethylene glycol) Incorporated Alginate, Chitosan, and Poly-l-lysine Microcapsules, Mol. Pharmaceutics 2 (2005) 29-36.

[54] A.J. García, Interfaces to Control Cell-Biomaterial Adhesive Interactions, in: C. Werner, editor, Polymers for Regenerative Medicine, 203 ed. Springer Berlin Heidelberg, 2006, pp. 171-190.

[55] G. Assero, C. Satriano, G. Lupo, C.D. Anfuso, G. Marletta, M. Alberghina, Pericyte adhesion and growth onto polyhydroxymethylsiloxane surfaces nanostructured by plasma treatment and ion irradiation, Microvas. Res. 68 (2004) 209-220.

[56] N.J. Hallab, K.J. Bundy, K.F. O'Connor, R.L. Moses, J.J. Jacobs, Evaluation of metallic and polymeric biomaterial surface energy and surface roughness characteristics for directed cell adhesion, Tissue Eng. 7 (2001) 55-71.

[57] F. Khan, S.R. Ahmad, Polysaccharides and their derivatives for versatile tissue engineering application, Macromol. Biosci. 13 (2013) 395-421.

[58] N. Berardi, T. Pizzorusso, L. Maffei, Extracellular matrix and visual cortical plasticity: freeing the synapse, Neuron 44 (2004) 905-908.

[59] B. Barrilleaux, P.S. Knoepfler, Inducing iPSCs to escape the dish, Cell Stem Cell 9 (2011) 103-111.

[60] K. Sugai, R. Fukuzawa, T. Shofuda, H. Fukusumi, S. Kawabata, Y. Nishiyama, Y. Higuchi, K. Kawai, M. Isoda, D. Kanematsu, T. Hashimoto-Tamaoki, J. Kohyama, A. Iwanami, H. Suemizu, E. Ikeda, M. Matsumoto, Y. Kanemura, M. Nakamura, H. Okano, Pathological classification of human iPSC-derived neural

stem/progenitor cells towards safety assessment of transplantation therapy for CNS diseases, Mol. Brain 9 (2016) 85.

[61] N.J. Lamas, B. Johnson-Kerner, L. Roybon, Y.A. Kim, A. Garcia-Diaz, H. Wichterle, C.E. Henderson, Neurotrophic requirements of human motor neurons defined using amplified and purified stem cell-derived cultures, PLoS One 9 (2014) e110324.

[62] H.J. Chung, W.H. Chung, J.H. Lee, D.J. Chung, W.J. Yang, A.J. Lee, C.B. Choi, H.S. Chang, D.H. Kim, H.J. Suh, D.H. Lee, S.H. Hwang, S. Do, H.Y. Kim, Expression of neurotrophic factors in injured spinal cord after transplantation of human-umbilical cord blood stem cells in rats, J. Vet. Sci. 17 (2016) 97–102.

[63] M.F. Iulita, A.C. Cuello, The NGF metabolic pathway in the CNS and its dysregulation in down syndrome and Alzheimer's disease, Curr. Alzheimer Res. 13 (2016) 53-67.

[64] G. Cappelletti, M. Galbiati, C. Ronchi, M.G. Maggioni, E. Onesto, A. Poletti, Neuritin (cpg15) enhances the differentiating effect of NGF on neuronal PC12 cells, J. Neurosci. Res. 85 (2007) 2702-2713.

[65] E. Karamoysoyli, R.C. Burnand, D.R. Tomlinson, N.J. Gardiner, Neuritin mediates nerve growth factor-induced axonal regeneration and is deficient in experimental diabetic neuropathy, Diabetes 57 (2008) 181-189.

[66] R. Gao, X. Li, S. Xi, H. Wang, H. Zhang, J. Zhu, L. Shan, X. Song, X. Luo, L. Yang, J. Huang, Exogenous neuritin promotes nerve regeneration after acute spinal cord injury in rats, Hum. Gene Ther. 27 (2016) 544-554.

[67] W. Zeng, M. Rong, X. Hu, W. Xiao, F. Qi, J. Huang, Z. Luo, Incorporation of Chitosan microspheres into collagen-Chitosan scaffolds for the controlled release of nerve growth factor, PLoS One 9 (2014) e101300.

[68] Y.Z. Zhao, X. Jiang, J. Xiao, Q. Lin, W.Z. Yu, F.R. Tian, K.L. Mao, W. Yang, H.L. Wong, C.T. Lu, Using NGF heparin-poloxamer thermosensitive hydrogels

to enhance the nerve regeneration for spinal cord injury, Acta Biomater. 29 (2016) 71-80.

[69] S.P. Zhu, Z.G. Wang, Y.Z. Zhao, J. Wu, H.X. Shi, L.B. Ye, F.Z. Wu, Y. Cheng, H.Y. Zhang, S. He, X. Wei, X.B. Fu, X.K. Li, H.Z. Xu, J. Xiao, Gelatin Nanostructured Lipid Carriers Incorporating Nerve Growth Factor Inhibit Endoplasmic Reticulum Stress-Induced Apoptosis and Improve Recovery in Spinal Cord Injury, Mol. Neurobiol. 53 (2016) 4375-4386.

**Figure Captions**

**Figure 1. Chitlac-based polymers are characterized by an increased surface polarity.**

Plots summarize in (A) the measured contact angles between water and polysaccharide-based surfaces and in (B) the Acid-Base work of adhesion for the different substrates.

**Figure 2. Hippocampal neurons display an enhanced growth and synaptic activity on Chitlac-THICK substrate.**

(A) Immunofluorescence micrographs of hippocampal cultures grown on Chitosan-THIN (left), Chitlac-THIN (middle) and Chitlac-THICK (right), labeled for the neuronal β-tubulin III (in red), the glial GFAP (in green) and the nuclei DAPI (in blue), markers. (B) Representative traces of spontaneous PSCs recorded from neurons grown on the three different substrates. Box plots summarize in (C) PSCs frequency and in (D) PSCs amplitude values measured from neurons grown on Chitosan-THIN (black), Chitlac-THIN (grey) and Chitlac-THICK (magenta). The dashed lines represent the mean values in all conditions. Note from Chitosan-THIN to Chitlac-THICK, the significant increase in PSCs frequency and amplitude. (E) Example of mPSCs recorded in the presence of TTX (1 μM) in Chitosan-THIN (top, black) and Chitlac-THICK (bottom, light grey). (F) Histograms showing that the significant

increase in PSCs frequency in Chitlac-THICK neurons is reflected also in the frequency of mPSCs. Scale bar: 50 μm in (A).

**Figure 3. fNPCs differentiate into MAP2-positive neurons preferentially on Chitlac-THICK substrate.**

(A) Fluorescence images of fNPCs grown on Chitosan-THIN (top), Chitlac-THIN (middle) and Chitlac-THICK (bottom), labeled for the neuronal marker β-tubulin III (in red) and the glial marker GFAP (in green). Nuclei are highlighted by DAPI in blue. Insets show β-tubulin III positive neurons at higher magnification. (B) Fluorescence images of fNPCs grown on Chitosan-THIN (top), Chitlac-THIN (middle) and Chitlac-THICK (bottom), labeled for the neuronal marker β-tubulin III (in red) and for the marker for mature neurons MAP2 (in green). Nuclei visualized by DAPI in blue. Insets show mature neurons double-positive for β-tubulin III and MAP2 at higher magnification. Scale bar: 100 μm and 50 μm (insets) in (A) and (B). Plot in (C) summarize the amount of β-tubulin III positive area vs GFAP one in the different substrates. Plot in (D) summarized the ratio of double positive MAP2 and β-tubulin III neurons in the three substrates.

**Figure 4. D7 differentiation is increased by Chitlac-THICK substrate.**

(A) GFAP (in green) and β-tubulin III (in red) immune-labeling on differentiated D7 progenitors cultured in the presence of MABs (D16), BDNF-expressing MABs (A9) and NGF-expressing MABs (F10) on the different substrates shows that D7 differentiate better when plated on Chitlac-THICK substrate, in particular in the presence of NGF, where more β-tubulin positive neurons are visible, compared to the other substrates. β-tubulin III and GFAP positive cells in (B) or ChAT positive cells in (C) quantified from D7 differentiated progenitors co-cultured with MABs (D16, A9 or F10) on the different substrates. When plated onto Chitlac-THICK substrate, D7 progenitors give rise to higher number of differentiated cells and produce more ChAT positive MN compared to Chitosan-THIN and Chitlac-THIN. In (D) β-tubulin III (in

red) and ChAT (in green) positive D7 differentiated cells on Chitlac-THICK in the presence of control MABs (D16, left panel), BDNF-MABs (A9, central panel) and NGF-MABs (F10, right panel), visible as GFP positive cells (in blue). Scale bar, 50 µm in (A) and (D).

**Figure 5. D16 MABs and A9 or F10 MABs further boost the synaptic activity of hippocampal neurons grown on Chitlac-THICK.**

(A) Fluorescence images of cultures grown on Chitlac-THICK: control hippocampal cells (control) or co-cultured with control MABs (D16), BDNF-expressing MABs (A9) or NGF-expressing MABs (F10), labeled for β-tubulin III (in red) and DAPI (in blue). MABs expressing GFP are represented in green. (B) Representative traces of spontaneous PSCs recorded from all conditions. In (C) box plots of PSCs frequency and in (D) of PSCs amplitude from neurons grown on Chitlac-THICK in the four different conditions. Note the strong increase in both parameters due to the presence of neurotrophins. Scale bar: 50 µm in (A).